

Self-interaction effects on charge-transfer collisions

Edwin E. Quashie,¹ Bidhan C. Saha,¹ Xavier Andrade,² and Alfredo A. Correa²

¹*Department of Physics, Florida A&M University, Tallahassee, FL 32307, USA*

²*Quantum Simulations Group, Lawrence Livermore National Laboratory, Livermore, California 94551, USA*

In this article, we investigate the role of the self-interaction error in the simulation of collisions using time-dependent density functional theory (TDDFT) and Ehrenfest dynamics. We compare many different approximations of the exchange and correlation potential, using as a test system the collision of $\text{H}^+ + \text{CH}_4$ at 30 eV. We find that semi-local approximations, like PBE, and even hybrid functionals, like B3LYP, produce qualitatively incorrect predictions for the scattering of the proton. This discrepancy appears because the self-interaction error allows the electrons to jump too easily to the proton, leading to radically different forces with respect to the non-self-interacting case. From our results, we conclude that using a functional that is self-interaction free is essential to properly describe charge-transfer collisions between ions and molecules in TDDFT.

I. INTRODUCTION

When a slow projectile collides with a molecular target, several microscopic dynamics, such as ro-vibrational excitations, dissociation, charge transfer, nuclear exchange and fragmentation occur during the process [1, 2]. These processes have received considerable attention in a wide range of applied fields, such as radiation therapy, material science, accelerators, plasma physics, chemistry and astrophysics [3–5]. At low incident energies, a large number of ion-molecule collisions experiments have been reported[6–9]; full understanding of these collision processes still poses challenges to both experiment and theory [10–13].

The development of practical methods for coupled molecular dynamics and real-time electron dynamics, in particular in the form of Ehrenfest dynamics [14–16] combined with time-dependent density functional theory (TDDFT) [17], have provided new effective tools for the study of atomic and molecular collisions with the predictive power of first principles methods [18–26].

As in all practical first-principles simulation methods, approximations are required to reduce the complexity of the full Schrödinger equation. The two major approximations in Ehrenfest-TDDFT are to approximate the dynamics of the ions as a single classical trajectory, and the use of an approximated exchange and correlation term in the TDDFT electron equations. In this paper we will focus on this second approximation, by comparing the results obtained by using different functionals for the same process. While TDDFT tends to get qualitatively good agreement with experimental results even with the most basic approximations to the exchange and correlation functional [27, 28], we find that for collision processes it becomes essential to use more advanced functionals that account for the self-interaction effects.

As a model system for our study we use the collision of a proton (H^+) with a methane molecule, which is a prototypical example at the intersection between the fields of chemistry and atomic collisions [29]. In ion-molecule collisions with proton has enjoyed wide applications, not only for its simplicity, but also for its ability to capture

electrons from the target. The process $\text{H}^+ + \text{CH}_4$ has been studied for $10 \leq E \leq 50$ eV by several groups. Toennies *et al.* [8, 11, 12], Udseth *et al.* [30], and Linder and Krutein [10] used a crossed-beam experiment to study inelastic and charge-transfer processes involving ion and molecule collisions. Rudd *et al.* [31] and McNeal [32] calculated total ionization cross sections in the energy range of $5 \leq E \leq 4000$ keV and $1 \leq E \leq 25$ keV respectively for proton-methane collision. Jacquemin *et al.* [33] calculated the differential cross section and integral cross sections and energy loss spectra for the process $\text{H}^+ + \text{CH}_4$ at 30 eV using an extended Lagrangian method (END). Gao *et al.* [34] investigated the dynamical evolution related to self-interaction correction (SIC) and calculated fragment intensity and intra-molecule energy transfer for $\text{H}^+ + \text{CH}_4$ at 30 eV.

II. THEORY

A fully quantum simulation of a collision process is not computationally feasible, so some approximations are essential. The most fundamental approximation is the separation of the electronic and nuclear degrees of freedom, which is justified by the large difference in mass between these two types of particles. Here we use the Ehrenfest approach [35], where the dynamics of the electrons are quantum, while the nuclei follow a classical Newtonian dynamics with forces given by the gradient of the instantaneous energy. The advantage of this approach is that the dynamics of the electrons are explicitly modeled, so that the simulation includes the excitation of the electrons due to the motion of the ions during the collision or by an external perturbation.

Even without the ionic degrees of freedom, simulating the full quantum dynamics of the electrons is rather impractical, so it requires further approximations. An efficient approach to do this simulations is the TDDFT framework [17, 36–38], where the many-body problem is mapped to the propagation of a non-interacting system.

The Ehrenfest-TDDFT equations are (atomic units are

used)

$$M_J \frac{\partial^2 \vec{R}_J}{\partial t^2} = - \frac{\partial E[n, \{\mathbf{R}_J(t)\}_J]}{\partial \vec{R}_J}, \quad (1)$$

$$i \frac{\partial}{\partial t} \varphi_i(\mathbf{r}, t) = \left\{ -\frac{\nabla^2}{2} + V_{\text{KS}}[n, \{\mathbf{R}_J(t)\}_J](\mathbf{r}, t) \right\} \varphi_i(\mathbf{r}, t), \quad (2)$$

where the electronic density is given by

$$n(\mathbf{r}, t) = \sum_i |\varphi_i(\mathbf{r}, t)|^2. \quad (3)$$

$\mathbf{R}_J(t)$ denotes the atomic coordinates evolving according to Ehrenfest forces [39], and φ_i are the electronic orbitals. The Kohn-Sham (KS) effective potential $V_{\text{KS}}[n](\mathbf{r}, t)$ is given as

$$V_{\text{KS}}[n, \{\mathbf{R}_J\}_J](\mathbf{r}, t) = V_{\text{ext}}[\{\mathbf{R}_J\}_J](\mathbf{r}, t) + V_{\text{H}}[n](\mathbf{r}, t) + V_{\text{xc}}[n](\mathbf{r}, t) \quad (4)$$

where $V_{\text{ext}}(\mathbf{r}, t)$ is the external potential due to ionic core potential and some possible external perturbations. $V_{\text{H}}[n](\mathbf{r}, t)$ is the Hartree potential which describes the classical electrostatic interactions between electrons, and $V_{\text{xc}}[n](\mathbf{r}, t)$ is the exchange-correlation (XC) potential.

The XC potential that corresponds to the Schrödinger equation is unknown in TDDFT, so this is the part that requires an approximation. The development of accurate and computationally efficient XC approximations remains a challenge in TDDFT, as this is one of the main sources of error in the theory [40–42].

The self-interaction error is one of the most well known deficiencies of the approximated functionals in both DFT and TDDFT. For N -electron systems, each electron must see an effective potential that corresponds to $N - 1$ electrons, otherwise each electron is effectively interacting electrostatically with itself. As the Hartree potential is the potential of N particles, to compensate, the exchange potential must behave like the potential of a hole and should decay as $-1/r$.

Many popular approximated density functionals, including the local density approximation (LDA) [43] and most generalized gradient approximations (GGAs), decay exponentially and do not correct for the self-interaction. The self-interaction error leads to systems that are too polarizable, as the effective KS potential is less attractive than it should be. This induces errors not only in the prediction of polarizabilities and hyperpolarizabilities [44], but also in ionization potentials [45, 46] and excitation energies [47, 48].

In order to overcome these errors, the first alternative is to use an exchange approximation that has the proper asymptotic limit. The exact exchange approach (EXX) [49, 50] is such a functional. It is, however, quite expensive computationally, especially if one wants to do non-adiabatic molecular dynamics. We can use the Krieger-Li-Iafrate (KLI) approximation [51] to reduce the

computational cost, while retaining the correct asymptotic limit. As this is an exchange functional, a proper accompanying correlation functional is not yet available.

It is also possible to find some semi-local functionals that have the proper asymptotic limit, in particular GGAs [52] and meta-GGAs [53, 54]. Hybrid functionals [55] still contain some level of self-interaction since they only include part of Hartree-Fock (HF) exchange (which is self-interaction free). To remove it completely, one must use more sophisticated range-separated hybrid functionals that include 100% exact exchange at long ranges [56].

There are several schemes that instead of proposing a functional, provide a way to modify an existing approximation in order to remove self interaction [57, 58]. The simplest approach is known as Fermi-Amaldi (FA) [59], and consists in simply scaling the Hartree potential by a factor $(N - 1)/N$. Although it corrects the asymptotic limit, it produces an exchange potential that is not very accurate elsewhere and it is not system-additive. An advanced version of this idea is the average-density self-interaction correction (ADSC) [60, 61] which includes additional terms to compensate the errors in the XC potential. Both FA and ADSC have a size-consistency problem which is important for collisions; if a system is composed of independent fragments they would provide a correct asymptotic limit for the whole system instead of each fragment.

In order to study the effect of the XC potential in collisions, we sample the results of different approximations. First, the standard Perdew-Burke-Ernzerhof (PBE) [62], and B3LYP [63] approximations that contain self-interaction. Second, we consider LDA with the self-interaction corrections (SIC) of FA and ADSC as mentioned earlier. Finally, we consider the exact exchange in the KLI approximation (EXX-KLI). We also tested EXX-KLI with the correlation functional from PBE and Lee-Yang-Parr (LYP) [64], however, we found no significant difference in the results with respect to EXX alone.

III. COMPUTATIONAL DETAILS

To evaluate the above time-dependent KS (TDKS) equation (Eq. 2) [65, 66] numerically, finite discretization of the functions φ_i as implemented in two different code packages called QBOX [67] and OCTOPUS [68, 69], were used for the numerical simulations.

In QBOX (with custom time-dependent modifications [70, 71]), a supercell approach is adopted with periodic boundary conditions and the wave functions are expanded in plane waves basis sets. In OCTOPUS, however, the TDKS equations are solved by discretizing all quantities in real space. (Details are given in Refs. [72–74].) These are two *independent* implementations of the same theory, which allows us to rule out effects due to implementation errors.

All relevant information regarding the detailed numeri-

cal implementation can be found in [67, 70, 75–78]. Thus, only a brief discussion of both procedures is presented here. In our present calculation various XC approximations are used. The accuracy of these approximations, however, becomes very important for effective description of collision dynamics processes.

Fig. 1 displays a schematic representation of the initial collisional geometry. The nuclei of the ground state CH_4 molecule consists of a carbon and four hydrogen atoms. There are, however, few different incident orientations of this system. Only one orientation as depicted in Fig. 1 is used in this calculation, which represents the initial orientation of $\text{H}^+ + \text{CH}_4$ before the collision process. This orientation is identical to the face II orientations of Jacquemin *et al.* [33] and Gao *et al.* [34] in which the incoming proton moves towards the methane from the negative-to-positive z-axis. The impact parameter b was increased in the positive x-axis. The C atom of methane is placed at the origin of the coordinates. The CH_4 molecule is initially at rest (laboratory reference). In order to avoid any prior interactions between the projectile and the methane we initially placed the H^+ at $(b, 0, -10 \text{ a.u.})$ from the CH_4 . Initially, the CH_4 is in its electronic ground state, calculated without the presence of the ion. The impact parameter b is varied in the range of $(0 - 7.0 \text{ } a_0)$ in steps of $\Delta b = 0.1 \text{ a.u.}$. The incoming proton initially is given a velocity of 0.0346 a.u. which corresponds to the kinetic energy $E = 30 \text{ eV}$. The total simulation time is 19.5 fs with a time step of $\Delta t = 0.838 \text{ attoseconds}$, the plane waves basis set are sampled with a 100 Ry energy cutoff and a numerical grid spacing of $0.3 \text{ } a_0$, for the respective codes, which are a converged value for all simulations described.

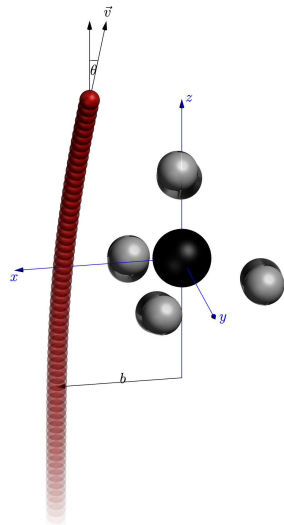


Figure 1. (color online). A schematic diagram for $\text{H}^+ + \text{CH}_4$ initial geometry. The red, gray, and black balls represent proton, hydrogen, and carbon respectively. The center of mass of the target is in the origin (on the carbon). θ denotes the scattering angle and b , the impact parameter.

IV. RESULTS AND DISCUSSION

We start our study by calculating the scattering angle θ as function of impact parameter b for different XC approximations, the results are shown in Fig. 2. Here we can already observe a significant difference between different XC functionals. B3LYP, PBE and LDA have a rough curve, with small scattering angles and two extrema. Self-interaction-corrected functionals FA, ADSIC, EXX have a completely different behavior, with a larger scattering angle and a single extrema.

If we assume that the interaction with the proton is attractive at long range and repulsive at short range, from molecular collision theory we can obtain some ideas of how the scattering angle should behave [79]. As CH_5^+ is a stable molecule [12], we expect the interaction between H^+ and CH_4 to exhibit such behavior.

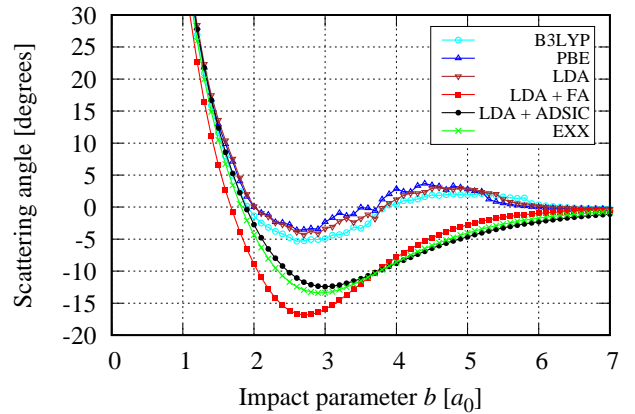


Figure 2. (color online). Scattering angle θ as a function of impact parameter b (real-space code) for different exchange-correlation functionals for Face II orientation. Sign is assigned to the angle according to the quadrant to which the proton scatters. This is to stress the attractive character of self-interaction and exact exchange theories but partially lost in the B3LYP, PBE and LDA theories.

For a small impact parameter the proton will scatter against the repulsive part of the potential, bouncing back and producing large scattering angles with a limit of 180 degrees for $0 \text{ impact parameter}$. This regime is observed in Fig. 2 for all functionals.

For higher impact parameters, the proton will probe the attractive region of the scattering potential and it will deflect towards the molecule (negative angles). As the impact parameter grows the interaction of the proton and the molecule becomes weaker, so we expect the scattering angle to have a maximum in this region. The value of this maximum is known as the *rainbow angle*, which corresponds to the maximum deflection angle for forward scattering.

In Fig. 2 we see that self-interaction-free functionals exhibit the behavior previously described, however B3LYP,

PBE and LDA show a second extrema of positive deflection. This suggests that a repulsive interaction is taking place at long ranges due to electronic self-interaction effects [80, 81].

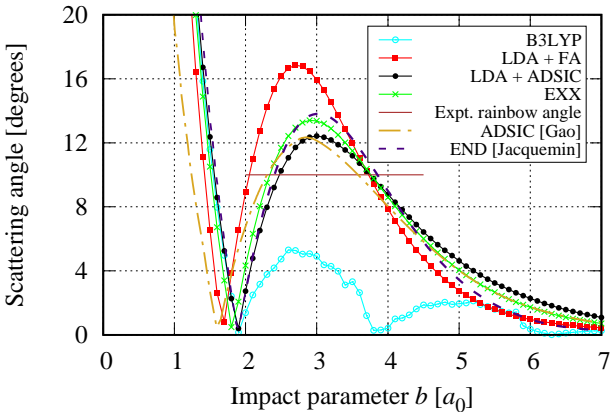


Figure 3. (color online). Scattering angle θ as a function of impact parameter b for different exchange-correlation functionals compared with theory (Jacquemin *et al.* [33] and Gao *et al.* [34]) for Face II orientation. Horizontal line is the experimentally determined rainbow angle over random orientations [12].

In order to further understand the difference in predictions, we compare our results for some of the XC functionals with available theoretical results (see Fig. 3). We also include in the plot the value of the rainbow angle that was measured experimentally by Chiu *et al.* [12] (the corresponding impact parameter is rather not measurable experimentally). The experimental rainbow angle was determined by averaging over all collision orientations while the theoretical results here are for single (Face II) orientation.

Table I compares different rainbow angle values. This comparison shows that B3LYP, PBE and LDA severely underestimate the experimental rainbow angle, showing that their results are qualitatively incorrect. LDA + FA, on the other hand, produces a maximum deflection angle that is 68% larger than the experimental value. Higher-level self-interaction-free approaches like LDA + ADSIC and EXX overestimate the rainbow angle too, but are closer in value with experiment.

To understand the nature of the repulsive regime in self-interacting functionals, we plot in Fig. 4 the charge on the proton as a function of time for $b = 3.0 a_0$. We define the charge on the proton using Bader charge analysis [82–84]. Fig. 5 shows snapshots of the distribution of the electronic charge density as a function of time for some of the functionals (PBE and EXX). From these figures it is observed that there is a significant difference in the charge transferred from the molecule to the proton between functionals.

For B3LYP and PBE, the charge q on the proton

	Rainbow angle [degrees]	Impact parameter [bohr]
Experimental (Average) [12]	10.0	–
B3LYP	6.8	2.7
PBE	3.6	2.7
LDA	4.3	2.7
LDA + FA	16.8	2.7
LDA + ADSIC	12.5	3.0
EXX	13.5	2.9
END [33]	14.4	3.0
ALDA + ADSIC [34]	12.3	2.8

Table I. Rainbow angles and the corresponding impact parameter where it is achieved. Comparison between the experimental result (the impact parameter is not accessible) and different theoretical models.

strongly oscillates, reaching a maximum value around $q = 1$. LDA + FA and EXX functionals have a very different behavior, there is a much smaller transfer of charge, with a maximum value around $q = 0.31$. In the case of LDA + ADSIC, there are oscillations in the charge, but they are smaller in amplitude and maximum value with respect to self-interacting functionals, which is not a surprising fact.

The effect of the self-interaction is to make it easier for the electron to escape the molecule, as the effective potential it sees is neutral; while the, more correct, self-interaction free effective potential corresponds to a system with charge -1 , which is more attractive for the proton.

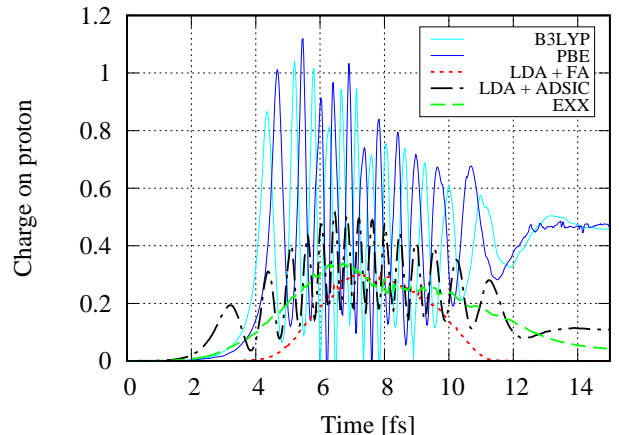


Figure 4. (color online). Evolution of Bader charge on the proton as a function of simulation time for $b = 3.0 a_0$ (real-space code).

In turn, this transfer of charge produces a strong difference in the resulting force between the proton and the molecule, and the ensuing deflection angle. This force is shown in Fig. 6. At long ranges, before the proton

	Charge on the proton [e]
B3LYP	0.4585
PBE	0.4668
LDA + FA	0.0003
LDA + ADSIC	0.1088
EXX	0.0414

Table II. Final charge on the proton after the collision event ($t = 15$ fs) for Face II orientation at $b = 3.0 a_0$. Charges were obtained using the Bader charge analysis [82, 83, 85].

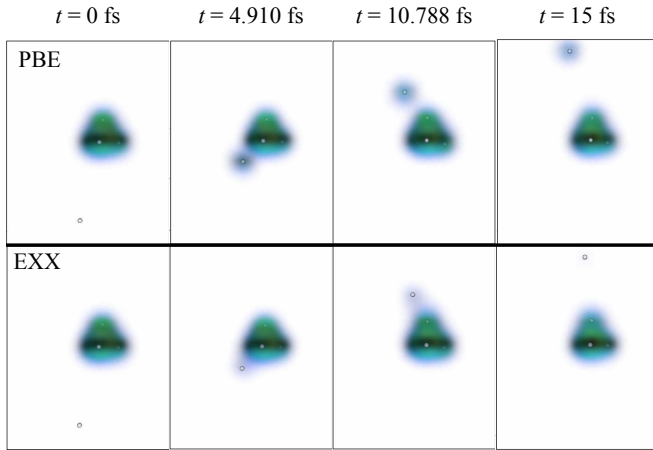


Figure 5. (color online). Snapshots of electronic charge density distribution of $\text{H}^+ + \text{CH}_4$ collision as a function of time for $b = 3.0 a_0$ for PBE and EXX (real-space code). The single gray ball represents the incoming H^+ and the middle balls with green-contour (charge density) represent the CH_4 atoms. H^+ interacts with the CH_4 charge density where some electron density is acquired during its trajectory and finally leaves CH_4 with some fraction of charges (see Table II). Orientation is the same as in Fig. 1. Plots produced using the VISIT visualization tool [86].

momentarily bounds to the molecule, the initial interaction is attractive; a charged particle is attracted by the dipole it induces in the molecule. However, when a certain amount of charge q is transferred to the proton, both parts of the system are positively charged and they repel each other with a force that is proportional to $q(1 - q)$.

This repulsive force produces the positive deflection angle regime that we observe at high impact parameters in Fig. 2 for both B3LYP and PBE. Moreover, since the charge in the proton oscillates, the force also does oscillate and changes sign. The effect of these oscillations is to reduce the overall deflection and produce the roughness observed in the scattering angle as a function of the impact parameter (Fig. 3).

The findings of LDA + FA show the opposite behavior to the self-interacting functionals, however, we think different mechanisms are at play in this case. The FA corrections add to the central region of the system an

attractive potential, which makes it harder for the electron to jump to the proton, reducing the level of charge transfer and avoiding the repulsive interaction. This attractive potential has other effects, too. It reduces the polarizability of the system, making the long range interaction smaller; for example, at time $t = 4$ fs in Fig. 6 the force in LDA + FA is about half of that due to LDA + ADSIC or EXX. For shorter ranges, however, LDA + FA strongly bounds the proton to the molecule, showing much larger forces than other functionals. This strong interaction explains the overestimation compared to the experimental rainbow angle.

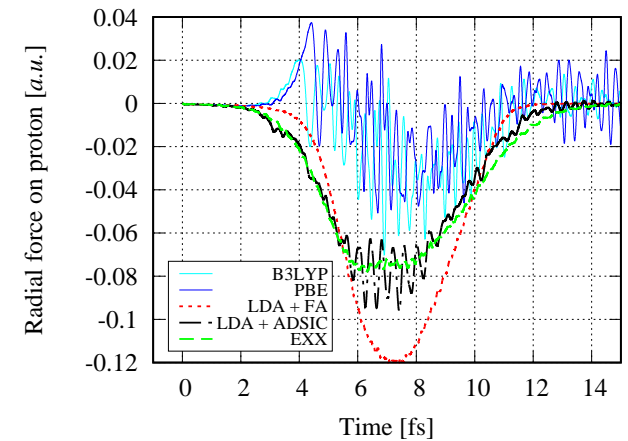


Figure 6. The radial force on proton as a function of simulation time for $b = 3.0 a_0$ (real-space code). Radial force is taken in the direction joining the central molecule to the moving proton. Negative values correspond to attractive forces.

Another result of our simulation is the remaining charge on the proton after the collision event, shown in Table II. While one would expect the final charge on the proton to be an integer, our simulations yield fractional charges [87]. This is not a limitation of the XC functional but a property of Ehrenfest dynamics. Ehrenfest is averaging over several potential energy surfaces that have different final charge state for the proton [88]. Therefore, we expect the final charge to reflect the probability distribution of the proton charge state that would be experimentally measured.

V. CONCLUSION

This paper reports our investigation on $\text{H}^+ + \text{CH}_4$ collision process at $E_{\text{lab}} = 30$ eV at a single orientation. Two separate code packages QBOX and OCTOPUS, which are independent Ehrenfest-TDDFT implementations, are used in this study for comparison and to confirm the effects induced by self-interaction effects in the electron and ion dynamics. The LDA, PBE and B3LYP functionals tend to produce trajectories sensitive to initial conditions and yield rugged differential cross sections due

to high frequency electronic oscillations. The inclusion of self-interaction corrections, even employing simple approximations like FA, yield smooth trajectories which are more comparable with previous HF-based results [33].

The different XC functionals studied in this investigation, grouped into SIC and non-SIC, are very sensitive to collision dynamics. The signatures of those approximations are explicitly visible in all our reported findings – scattering angle, forces and charges.

It is not hard to imagine that the spurious effects we see due to self-interaction are not a feature exclusive of the $H^+ + CH_4$ collision. We expect that similar effects would be observed in other systems. This allows us to theorize that in all cases that involve charge-transfer collisions, it is necessary to use self-interaction-free functionals or to include an ad-hoc correction term. This is necessary to correctly describe the binding of the outermost electron, and avoid too much, or too little, charge to move to the ion, changing the nature of the ion-molecule interaction. Fortunately, simple approximations like ADSIC improve considerably the results of self-interacting potentials with a negligible increment in the computational cost. We believe that this property allows Ehrenfest-TDDFT to of

fer a good tradeoff between accuracy and computational cost for the simulation of molecular collisions, in particular for large systems that are not accessible to more accurate theories.

VI. ACKNOWLEDGMENTS

Authors are thankful to Professor C. A. Weatherford, Dr. E. R. Schwegler, Dr. G. Avendaño-Franco and Dr. K. J. Reed for many useful discussions. This is a joint project between the Department of Physics, Florida A&M University and Lawrence Livermore National Laboratory. This work was performed under the auspices of the U.S. Department of Energy by Lawrence Livermore National Laboratory under Contract DE-AC52-07NA27344. Computing support for this work came from the Lawrence Livermore National Laboratory Institutional Computing Grand Challenge program. E. E. Quashie and B. C. Saha thankfully acknowledge the support by National Nuclear Security Administration (NNSA), Award Number(s) de-na0002630.

[1] H. Udseth, C. F. Giese, and W. R. Gentry, *Phys. Rev. A* **8**, 2483 (1973).

[2] C. Barnett, J. Ray, E. Ricci, M. Wilker, E. McDaniel, E. Thomas, and H. Gilbody, *Atomic data for controlled fusion research*, Tech. Rep. (1977).

[3] M. R. C. McDowell, in *Atomic and Molecular Processes in Controlled Thermonuclear Fusion* (Springer US, 1980) pp. 1–13.

[4] R. McCarroll, in *Atomic and Molecular Collision Theory* (Springer Science + Business Media, 1982) pp. 165–231.

[5] A. Salehzadeh and T. Kirchner, *Physics Procedia* **66**, 16 (2015).

[6] W. Gentry, H. Udseth, and C. F. Giese, *Chemical Physics Letters* **36**, 671 (1975).

[7] M. Noll and J. P. Toennies, *The Journal of Chemical Physics* **85**, 3313 (1986).

[8] G. Niedner, M. Noll, and J. P. Toennies, *The Journal of Chemical Physics* **87**, 2067 (1987).

[9] N. Aristov, G. Niedner-Schatteburg, J. P. Toennies, and Y.-N. Chiu, *The Journal of Chemical Physics* **95**, 7969 (1991).

[10] J. Krutein and F. Linder, *J. Chem. Phys.* **71**, 599 (1979).

[11] B. Friedrich, G. Niedner, M. Noll, and J. P. Toennies, *The Journal of Chemical Physics* **87**, 5256 (1987).

[12] Y.-N. Chiu, B. Friedrich, W. Maring, G. Niedner, M. Noll, and J. P. Toennies, *The Journal of Chemical Physics* **88**, 6814 (1988).

[13] N. Aristov, W. Maring, G. Niedner-Schatteburg, J. P. Toennies, Y.-N. Chiu, and H. Köppel, *The Journal of Chemical Physics* **99**, 2682 (1993).

[14] H. J. Lüddecke, in *Many-Particle Quantum Dynamics in Atomic and Molecular Physics* (Springer Science + Business Media, 2003) pp. 205–220.

[15] C. M. Isborn, X. Li, and J. C. Tully, *The Journal of Chemical Physics* **126**, 134307 (2007).

[16] A. Castro and E. K. U. Gross, *Journal of Physics A: Mathematical and Theoretical* **47**, 025204 (2014).

[17] E. Runge and E. K. U. Gross, *Phys. Rev. Lett.* **52**, 997 (1984).

[18] U. Saalmann and R. Schmidt, *Fortschritz Für Physik D Atoms Molecules and Clusters* **38**, 153 (1999).

[19] K. Yabana, T. Tazawa, Y. Abe, and P. Božek, *Phys. Rev. A* **57**, R3165 (1998).

[20] R. Nagano, K. Yabana, T. Tazawa, and Y. Abe, *J. Phys. B: At. Mol. Opt. Phys.* **32**, L65 (1999).

[21] R. Nagano, K. Yabana, T. Tazawa, and Y. Abe, *Phys. Rev. A* **62** (2000), 10.1103/physreva.62.062721.

[22] X.-M. Tong, T. Watanabe, D. Kato, and S. Ohtani, *Phys. Rev. A* **66** (2002), 10.1103/physreva.66.032709.

[23] N. Henkel, M. Keim, H. J. Lüddecke, and T. Kirchner, *Phys. Rev. A* **80** (2009), 10.1103/physreva.80.032704.

[24] F. Wang, X. Xu, X. Hong, J. Wang, and B. Gou, *Physics Letters A* **375**, 3290 (2011).

[25] G. Avendaño-Franco, B. Piroux, M. Grüning, and X. Gonze, *Theor Chem Acc* **131** (2012), 10.1007/s00214-012-1289-5.

[26] X. Hong, F. Wang, Y. Wu, B. Gou, and J. Wang, *Phys. Rev. A* **93** (2016), 10.1103/physreva.93.062706.

[27] E. Engel and R. M. Dreizler, in *Theoretical and Mathematical Physics* (Springer Science + Business Media, 2010) pp. 109–217.

[28] T. Tsuneda, in *Density Functional Theory in Quantum Chemistry* (Springer Science + Business Media, 2014) pp. 101–124.

[29] B. H. Bransden, M. R. C. McDowell, and E. J. Mansky, *Physics Today* **46**, 124 (1993).

[30] J. M. Udseldr, *Brugheant Phys.* **60**, 3051 (1974).

[31] M. E. Rudd, R. D. DuBois, L. H. Toburen, C. A. Ratcliffe, and T. V. Goffe, *Physical Review A* **28**, 3244 (1983).

[32] R. J. McNeal, *J. Chem. Phys.* **53**, 4308 (1970).

[33] D. Jacquemin, J. A. Morales, E. Deumens, and Y. Öhrn, *The Journal of Chemical Physics* **107**, 6146 (1997).

[34] C.-Z. Gao, J. Wang, F. Wang, and F.-S. Zhang, *The Journal of Chemical Physics* **140**, 054308 (2014).

[35] Z. Phys. **45**, 455 (1927).

[36] E. K. U. Gross, C. A. Ullrich, and U. J. Gossmann, in *Density Functional Theory* (Springer Science + Business Media, 1995) pp. 149–171.

[37] C. A. Ullrich, in *Concepts and Applications* (Oxford University Press, 2011) pp. 213–251.

[38] A. Harker, *Contemporary Physics* **54**, 55 (2013).

[39] X. Andrade, A. Castro, D. Zueco, J. L. Alonso, P. Echenique, F. Falceto, and Á. Rubio, *J. Chem. Theory Comput.* **5**, 728 (2009).

[40] T. Gould and J. F. Dobson, *The Journal of Chemical Physics* **138**, 014103 (2013).

[41] Y. Liu and J. Wu, *Phys. Chem. Chem. Phys.* **16**, 16373 (2014).

[42] A. O. de-la Roza, G. A. DiLabio, and E. R. Johnson, *J. Chem. Theory Comput.* **12**, 3160 (2016).

[43] W. Kohn and L. J. Sham, *Phys. Rev.* **140**, A1133 (1965).

[44] X. Andrade, S. Botti, M. A. L. Marques, and A. Rubio, *The Journal of Chemical Physics* **126**, 184106 (2007).

[45] R. Merkle, A. Savin, and H. Preuss, *Chemical Physics Letters* **194**, 32 (1992).

[46] K. Watanabe, *The Journal of Chemical Physics* **26**, 542 (1957).

[47] C. V. Caillie and R. D. Amos, *Chemical Physics Letters* **317**, 159 (2000).

[48] M. Levy, *Phys. Rev. A* **52**, R4313 (1995).

[49] F. D. Sala and A. Görling, *Int. J. Quantum Chem.* **91**, 131 (2002).

[50] H. O. Wijewardane and C. A. Ullrich, *Phys. Rev. Lett.* **100** (2008), 10.1103/physrevlett.100.056404.

[51] J. Krieger, Y. Li, and G. Iafrate, *Physics Letters A* **146**, 256 (1990).

[52] R. van Leeuwen and E. J. Baerends, *Phys. Rev. A* **49**, 2421 (1994).

[53] A. D. Becke and E. R. Johnson, *The Journal of Chemical Physics* **123**, 154101 (2005).

[54] E. Räsänen, S. Pittalis, and C. R. Proetto, *The Journal of Chemical Physics* **132**, 044112 (2010).

[55] A. D. Becke, *The Journal of Chemical Physics* **98**, 1372 (1993).

[56] H. Iikura, T. Tsuneda, T. Yanai, and K. Hirao, *The Journal of Chemical Physics* **115**, 3540 (2001).

[57] J. P. Perdew and A. Zunger, *Phys. Rev. B* **23**, 5048 (1981).

[58] X. Andrade and A. Aspuru-Guzik, *Phys. Rev. Lett.* **107** (2011), 10.1103/physrevlett.107.183002.

[59] E. Fermi and E. Amaldi, *Accad. Ital. Rome.* **6** (1934).

[60] S. Kümmel and L. Kronik, *Reviews of Modern Physics* **80**, 3 (2008).

[61] C. Legrand, E. Suraud, and P.-G. Reinhard, *J. Phys. B: At. Mol. Opt. Phys.* **35**, 1115 (2002).

[62] J. P. Perdew, K. Burke, and M. Ernzerhof, *Phys. Rev. Lett.* **77**, 3865 (1996).

[63] P. J. Stephens, F. J. Devlin, C. F. Chabalowski, and M. J. Frisch, *The Journal of Physical Chemistry* **98**, 11623 (1994).

[64] C. Lee, W. Yang, and R. G. Parr, *Phys. Rev. B* **37**, 785 (1988).

[65] C. A. Ullrich, *Time-Dependent Density-Functional Theory* (Oxford University Press (OUP), 2011).

[66] M. A. Marques, C. A. Ullrich, F. Nogueira, A. Rubio, K. Burke, and E. K. U. Gross, eds., *Time-Dependent Density Functional Theory* (Springer Berlin Heidelberg, 2006).

[67] F. Gygi, *IBM Journal of Research and Development* **52**, 137 (2008).

[68] A. Castro and M. Marques, in *Time-Dependent Density Functional Theory* (Springer Science + Business Media, 2006) pp. 197–210.

[69] X. Andrade, D. Strubbe, U. D. Giovannini, A. H. Larsen, M. J. T. Oliveira, J. Alberdi-Rodriguez, A. Varas, I. Theophilou, N. Helbig, M. J. Verstraete, L. Stella, F. Nogueira, A. Aspuru-Guzik, A. Castro, M. A. L. Marques, and A. Rubio, *Phys. Chem. Chem. Phys.* **17**, 31371 (2015).

[70] A. Schleife, E. W. Draeger, Y. Kanai, and A. A. Correa, *J. Chem. Phys.* **137**, 22A546 (2012).

[71] E. W. Draeger, X. Andrade, J. A. Gunnels, A. Bhatele, A. Schleife, and A. A. Correa, in *2016 IEEE International Parallel and Distributed Processing Symposium* (Institute of Electrical & Electronics Engineers (IEEE), 2016).

[72] A. Rubio, J. A. Alonso, X. Blase, L. C. Balbás, and S. G. Louie, *Phys. Rev. Lett.* **77**, 247 (1996).

[73] J. R. Chelikowsky, N. Troullier, and Y. Saad, *Phys. Rev. Lett.* **72**, 1240 (1994).

[74] I. Vasiliev, S. Öğüt, and J. R. Chelikowsky, *Phys. Rev. Lett.* **82**, 1919 (1999).

[75] M. Marques, *Computer Physics Communications* **151**, 60 (2003).

[76] A. Castro, M. A. L. Marques, and A. Rubio, *The Journal of Chemical Physics* **121**, 3425 (2004).

[77] X. Andrade, J. Alberdi-Rodriguez, D. A. Strubbe, M. J. T. Oliveira, F. Nogueira, A. Castro, J. Muguerza, A. Arruabarrena, S. G. Louie, A. Aspuru-Guzik, A. Rubio, and M. A. L. Marques, *Journal of Physics: Condensed Matter* **24**, 233202 (2012).

[78] X. Andrade and A. Aspuru-Guzik, *J. Chem. Theory Comput.* **9**, 4360 (2013).

[79] M. S. Child and P. Pechukas, *Phys. Today* **29**, 59 (1976).

[80] T. Schmidt, E. Kraisler, A. Makkal, L. Kronik, and S. Kümmel, *The Journal of Chemical Physics* **140**, 18A510 (2014).

[81] O. V. Gritsenko, L. M. Mentel, and E. J. Baerends, *The Journal of Chemical Physics* **144**, 204114 (2016).

[82] A. Arnaldsson, W. Tang, S. Chill, W. Chai, and G. Henkelman, *Bader Charge Analysis*, <http://theory.cm.utexas.edu/bader/>.

[83] R. F. W. Bader, *Chemical Reviews* **91**, 893 (1991).

[84] M. Yu and D. R. Trinkle, *The Journal of Chemical Physics* **134**, 064111 (2011).

[85] Y. Wang, T. Gould, J. F. Dobson, H. Zhang, H. Yang, X. Yao, and H. Zhao, *Phys. Chem. Chem. Phys.* **16**, 1424 (2014).

[86] H. Childs, E. Brugger, B. Whitlock, J. Meredith, S. Ahern, D. Pugmire, K. Biagas, M. Miller, C. Harrison, G. H. Weber, H. Krishnan, T. Fogal, A. Sanderson, C. Garth, E. W. Bethel, D. Camp, O. Rübel, M. Durant, J. M. Favre, and P. Navrátil, in *High Performance Visualization—Enabling Extreme-Scale Scientific Insight* (2012) pp. 357–372.

[87] M. E. Madjet, F. El-Mellouhi, M. A. Carignano, and G. R. Berdiyorov, *J. Appl. Phys.* **119**, 165501 (2016).

[88] J. C. Tully, *The Journal of Chemical Physics* **93**, 1061 (1990).